Physics and Imaging in Radiation Oncology 16 (2020) 138–143

Contents lists available at ScienceDirect

Physics and Imaging in Radiation Oncology

journal homepage: www.sciencedirect.com/journal/physics-and-imaging-in-radiation-oncology

Imaging prior to radiotherapy impacts *in-vitro* survival

Peter L. Kench [a], Linda Rogers [b,c], Ana Esteves [a], Tina Gorjiara [b,d], Elizabeth Claridge Mackonis [b,c], Stephen Morrell [e], David R. McKenzie [b,c], Natalka Suchowerska [b,c,*]

[a] Discipline of Medical Imaging Science and Brain and Mind Centre, Faculty of Medicine and Health, University of Sydney, NSW 2006, Australia
[b] VectorLAB, Radiation Oncology, Chris O'Brien Lifehouse, Missenden Rd, Camperdown, Sydney, NSW 2050, Australia
[c] University of Sydney, School of Physics, NSW 2006, Australia
[d] GenesisCare, Department of Radiation Oncology, The Mater Hospital, Crows Nest, NSW 2065, Australia
[e] University of New South Wales, School of Public Health and Community Medicine, NSW 2052, Australia

ARTICLE INFO

Keywords:
CBCT
Radiation therapy
Imaging dose
Clonogenic survival

ABSTRACT

Background and purpose: Cone Beam Computed Tomography (CBCT) is routinely used in radiotherapy to identify the position of the target volume. The aim of this study was to determine whether the CBCT dose, when followed by the treatment, influences the therapeutic outcomes as determined by in-vitro clonogenic cell survival in a radiobiological experiment.
Materials and methods: Human cell lines, four cancer and one normal, were exposed to a 6 MV photon beam, produced by a linear accelerator. For half of each sample, a prior imaging dose was delivered using the on-board CBCT. A sample size of n = 103 was used to achieve statistical power.
Results: The experimental group of cell lines exposed to CBCT imaging prior to treatment exhibited a reduction in mean cancer cell survival of ~17 times ($p = 0.02$) greater than predicted from the average dose response and equivalent to more than 5% of the therapeutic dose, compared to 11 times greater than predicted for normal cells (n.s.).
Conclusion: The greater than predicted reduction in survival resulting from the additional CBCT dose is consistent with radiation-induced bystander effects.

1. Introduction

Cancer patients undergoing radiotherapy are exposed to an imaging dose to provide confidence to advance to the boundaries of safe treatment, enabling the delivery of high doses per fraction using adaptive, stereotactic and gated treatments [1–3]. Most in-treatment imaging is performed using cone-beam computed tomography (CBCT) on the assumption that geometric validation of the treatment outweighs the risks of the additional dose, reported to be between 0.04 cGy and 3.62 cGy [4,5]. Despite the relatively low dose, Cheng et al. predict an increase in secondary cancers of 0.8% from a single high quality CBCT of the head and neck [6]. Even a small adverse effect could be significant across multiple fractions and large numbers of patients.

The CBCT dose has the potential to increase deterministic and stochastic effects [7]. Although there is discussion on whether to include the dose from the CBCT into the treatment plan calculations [8,9], this is not routinely performed. Studies have determined the imaging dose from CBCT with Monte Carlo simulations [10], but a biological endpoint suitable to quantify the effects of the dose contribution from CBCT on treatment outcomes has not yet been proposed. If an interaction between imaging dose and therapeutic dose exists, then this needs to be considered in the design of the treatment protocol. Furthermore, the small radiation dose from imaging may lead to low dose hyper-radiosensitivity [11,12] or it may induce radiation hormesis, manifesting as an increase in the survival of cells [13,14].

Some studies examine the effect of a small dose followed by a subsequent larger dose. Lin and Wu [15] report on eleven cell lines receiving different sequences of small (10 to 50 cGy) and large partial fractions to a total dose of 2 Gy, finding a cell survival reduction when the small dose preceded the larger dose. More recently, Yan et al. [16] have used this argument to support an ongoing prospective clinical trial (NCT03061162) for pulsed low dose rate radiotherapy, delivering 10

* Corresponding author at: VectorLAB, Radiation Oncology, Chris O'Brien Lifehouse, Sydney, NSW, Australia.
E-mail address: natalka.suchowerska@lh.org.au (N. Suchowerska).

https://doi.org/10.1016/j.phro.2020.11.003
Received 22 May 2020; Received in revised form 8 November 2020; Accepted 9 November 2020
Available online 28 November 2020

fractions of 0.2 Gy to a total of 2 Gy in 30 min. In a pooled study of two cancer cell lines and one normal epithelial cell line, it was found that a dose of 14 cGy corresponding to a 4DCT imaging dose, resulted in a statistically significant reduction in cell survival when preceding a therapeutic dose [17]. However, the study did not have sufficient statistical power to detect an effect with a CBCT dose of only 0.6 cGy.

The present study is aimed to test the hypothesis that the dose from CBCT imaging in addition to a therapeutic dose causes a change in the survival of cells compared to a therapeutic dose alone. Our study was designed to detect the biological effect of an additional small dose contribution, typical of a CBCT dose. The cell lines were selected to represent a broad range of radiosensitivities.

2. Materials and methods

Four human cancer cell lines and one normal, were selected as tissues frequently subjected to imaging in radiotherapy (Table 1). The cell lines, obtained from American Type Culture Collection (ATCC) and CellBank Australia, were cultured in a humidified incubator with 5% CO_2 at 37 °C, according to the manufacturers' instructions, and allowed to reach 80% confluence. Cell cultures were maintained at passage numbers lower than 15. No antibiotics or antifungal agents were used to minimize stress on cells [18].

2.1. Clonogenic survival

The clonogenic cell survival assay (Franken et al. [19]), was used to evaluate the effects of radiation. Exponentially growing cells were harvested (0.05% trypsin-EDTA solution, 4–6 min at 37 °C, centrifuged at 125 × *g* for 6 min) and seeded in 5 mL of growth medium in T25 cm^2 flasks (Corning, MA, USA) at previously optimized cell densities (Supplementary Table 1). The cells were allowed to adhere by incubating overnight and flasks were topped up to 10 mL of growth medium for appropriate backscatter volume.

Following irradiation, the cells were incubated at 37 °C, 5% CO_2 for pre-determined periods allowing colonies greater than 50 cells to form. Cell densities and number of incubation days were predetermined to optimise plating efficiency (Supplementary Table 1).

Cell colonies were fixed and stained. The selection of the staining and fixation agents was based on the dispersion and attachment of colonies to the flask surface (Supplementary Table 1). After 60 min, excess stain was removed and flasks were washed in water and dried in a ventilated oven at 35–40 °C.

Flasks were scanned using 205 dpi spatial resolution with ColCount™ (Oxford Optronix Ltd., Abingdon, UK). The colony counts for irradiated flasks were normalized to the un-irradiated controls (sham exposed) to determine the survival fraction.

2.2. Radiation exposure

To establish the dose response of each of the cell lines, they were exposed to a dose in the range 0 to 10 Gy with a uniform 6 MV photon beam at a dose-rate of 6 Gy/min on a Varian Novalis™ linear accelerator. Full scatter conditions were achieved by placing the six T25 flasks in a square Perspex phantom (Fig. 1A), sandwiched between blocks of

Table 1
Human cell lines chosen for this study, the tissue of origin and the type of cancer/disease.

Cell Line	Tissue of origin	Disease
NCI-H460 (ATCC® HTB-177™)	Lung: pleural effusion	Carcinoma; large cell lung cancer
DU 145 (ATCC® HTB81™)	Prostate; derived from metastatic site: brain	Carcinoma
CAL 27 (ATCC® CRL2095™)	Tongue	Squamous cell carcinoma
Hs 683 (ATCC® HTB138™)	Brain	Glioma
PNT1A (CellBank Australia 95012614)	Prostate, human post pubertal, immortalized with SV40	Normal

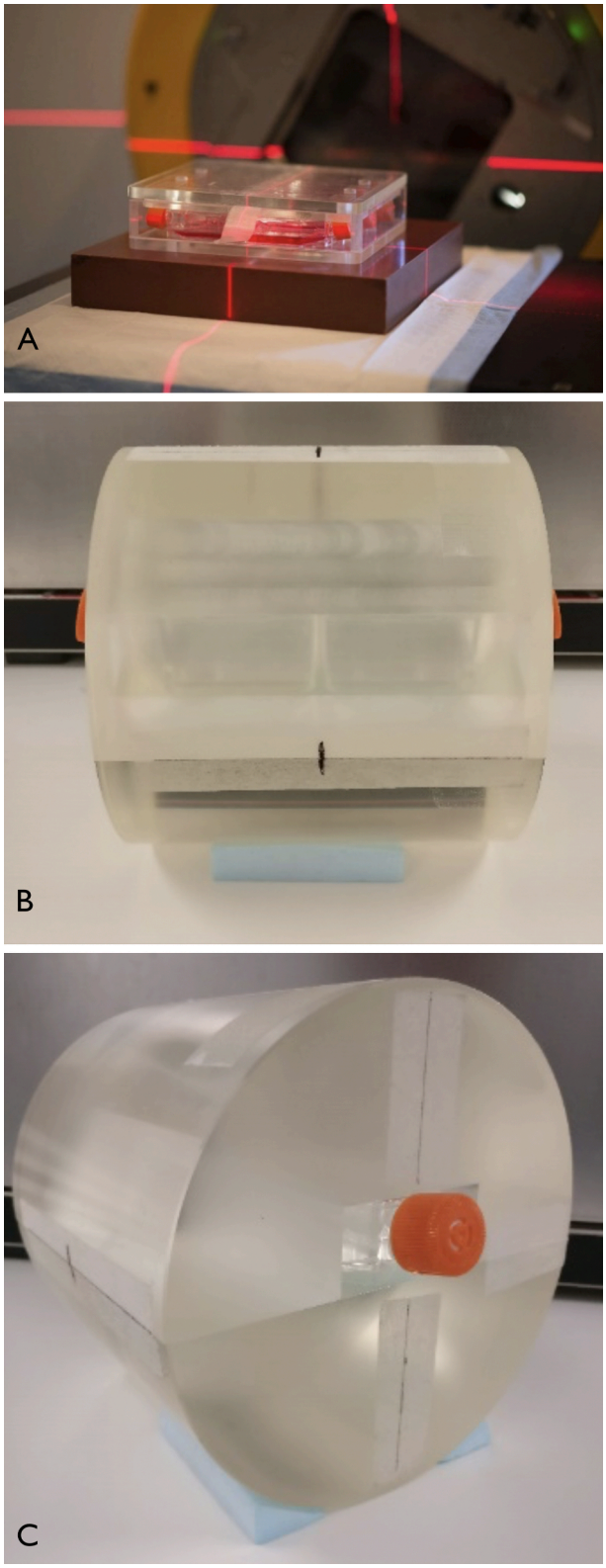

Fig. 1. (A) Perspex square phantom to establish the dose response. (B and C) Customised cylindrical phantom for cell exposure to 3-field treatment and CBCT.

Solid Water™ locating the cell layer at a depth of 50 mm. The accelerator gantry was set to 180° and the field size was 30 × 30 cm. The dose to the cells was independently confirmed using film dosimetry as previously described by Claridge Mackonis, et al. [20]. All flasks were kept in a thermally insulated container except when being irradiated and returned to the incubator immediately after exposure. Sham exposed flasks were prepared for each experiment and used as controls.

A dose response curve was generated to characterise the radiosensitivity of each cell line. For each experiment, the average survival fraction from 6 flasks was calculated (technical replicates). The survival fraction for each flask, for each cell line from 3 to 7 separate biological experiments (biological replicates, $n > 18$ for each dose and cell line) were fitted with the linear-quadratic (LQ) model. For each cell line, at least three experiments were carried out on separate occasions and the survival fractions combined to form a single distribution. Alpha and beta parameters were estimated using the maximum likelihood estimation method as defined by the CFAssay package for R [21]. A 0.50 survival fraction was selected to place observations in a sensitive region of the response curve and was determined using the alpha and beta parameters for each cell line (Table 2). The slopes of the survival curves are approximately equal at the 0.5 survival dose, allowing us to obtain similar response for each cell line for the same increment in dose. The reason for doing this is to enable the differences in survival between cancer cells of different cell lines receiving the therapy dose alone and those receiving the therapy dose and an additional imaging dose to form a normal distribution.

Combined CBCT and therapy exposures were carried out using a cylindrical phantom, diameter 160 mm (Fig. 1B and C), customised to house two T25 culture flasks simultaneously, positioning the cell layer at the axis of the phantom. The phantom was designed to insert into a CTDI phantom [29] for larger separations when simulating the pelvis. Here the phantom was used alone. A three-field plan was calculated on the Varian Eclipse v13.6 to deliver the prescribed dose to each cell line in the culture flask. Identical cylindrical phantoms were built to perform dosimetry with a thimble ionisation chamber and radiochromic film.

For each cell line and each experimental session, the culture flasks were divided into two groups: those receiving the three field treatment alone (T) with a separation of 1 min between each field and those exposed to the 'standard head CBCT' option on the Varian Novalis (CBCT), 3 min prior to the treatment described above. We also performed a substudy of CBCT only.

2.3. Dosimetry

The dose delivered with the CBCT and the 3-field treatment were independently verified. Radiochromic film (Gafchromic XRQA2) was located in the phantom at the cell layer to determine the dose from the CBCT (Fig. 1B). A Varian standard head CBCT was taken six times to provide sufficient dose to the film for three film replicates. Films were scanned after 24 h (Epson XL 10000: reflective mode; 48-bit colour; 72 dpi).

A calibration curve was created using a Pantak Kilovoltage unit, selecting a beam quality to best match the CBCT beam. Films were analysed in ImageJ (National Institute of Health, USA). For improved low dose accuracy, a calibration curve was created for the dose range 1–20 cGy. This calibration curve enabled the mean CBCT dose to be determined.

For the treatment delivered with a 6MV beam, film dosimetry was performed with Gafchromic EBT3 film, which is designed for use in the MeV energy range. The film was located in the position of the cells and exposed to the 3-field treatment plan. A calibration curve was established using a range of known doses. The films were processed as described, but read in transmission mode.

Table 2
The alpha and beta values for each cell line, calculated from the radiation survival curves using the linear quadratic model of fitting.

Cell Line	alpha (α)	beta (β)	Dose for 50% survival (Gy)	Theoretical reduction for CBCT dose 0.66 cGy (%)
NCI-H460	0.052	0.0484	3.0	0.23
DU 145	0.166	0.0298	2.5	0.21
CAL 27	0.200	0.0484	2.5	0.29
Hs 683	2.339	5.303	3.0	0.16
PNT1A	0.0591	0.0573	3.0	0.27

2.4. Statistical analysis

To test the hypotheses, the approach we used in our statistical analysis was to test the distribution of differences in survival fractions between the T exposure and the CBCT + T exposure for normality. The normality tests used were the D'Agostino & Pearson omnibus, Shapiro-Wilk, Kolmogorov-Smirnov, Cramer-von Mises and Anderson-Darling tests with Graphpad Prism v6 or Statistical Analysis Software (SAS, version 9.4). Where the distributions satisfied the normality criteria, paired two-tailed t-tests were performed to determine statistical significance. The hypothesis for testing was that imaging dose caused a change in cell survival. Statistically significant differences were defined at a level of $p < 0.05$. As the cells in each experiment are genetically identical, the statistical significance of mean differences in survival fractions between the control and experimental groups was tested using paired t-tests. Our experimental design and statistical analysis control for the fact that we have a range of cell lines in our study.

Since there are multiple combinations of flasks that could be used within each experiment to form differences, a Monte Carlo approach was used to randomise the possible combinations. The Monte Carlo process conducted 10,000 random combinations (over 1.29 million records in total) within each experiment for each cell line. The median p-value from the 10,000 t-tests was then taken as the (two-tailed) significance level. The Monte Carlo randomisation and repeated t-tests were performed using SAS 9.4.

3. Results

The measured dose response for each cell line is shown in Fig. 2. From this figure it can be seen that this study included a radio-resistant glioma (Hs 683) cell line and a radiosensitive tongue (CAL 27) cell line, with all other cell lines showing radiosensitivities between these two cases.

The measured CBCT imaging dose was 0.66 cGy. The calculated expected mean reduction in survival across all cell lines (0.00116) and across all cancers (0.00112) was determined using the experimentally derived alpha and beta parameters with equal weighting given to each cell line (Table 2). A substudy of CBCT alone produced no differences in survival fractions from the unirradiated control (results not shown). There was no significant difference in survival ($p < 0.05$) between any pair of (T) and (CBCT + T) for individual cell lines as shown in Supplementary Fig. S1.

All distributions of differences passed the normality tests (Supplementary Table 2), permitting the use of the statistical paired *t*-test. The difference of the paired survival fractions for (T) and for (CBCT + T), as frequency distribution histograms, are shown in Fig. 3 ($n = 103$) for all cancer cell lines for one random pairing. The mean of the distribution (the most probable value) was clearly above zero with a significance of $p = 0.014$, indicating that the CBCT imaging dose significantly reduced survival. The results of the Monte-Carlo paired t-tests confirmed the difference in survival fractions for cancer cells was significant ($p = 0.03$; $n = 103$ flasks). No significance was found for non-cancer (normal) cells ($p = 0.53$; $n = 26$ flasks).

Using the experimentally derived alpha and beta parameters in Table 2, the reduction in survival ((T) – (CBCT + T)), for an incremental increase in dose corresponding to the 0.66 cGy imaging dose, was

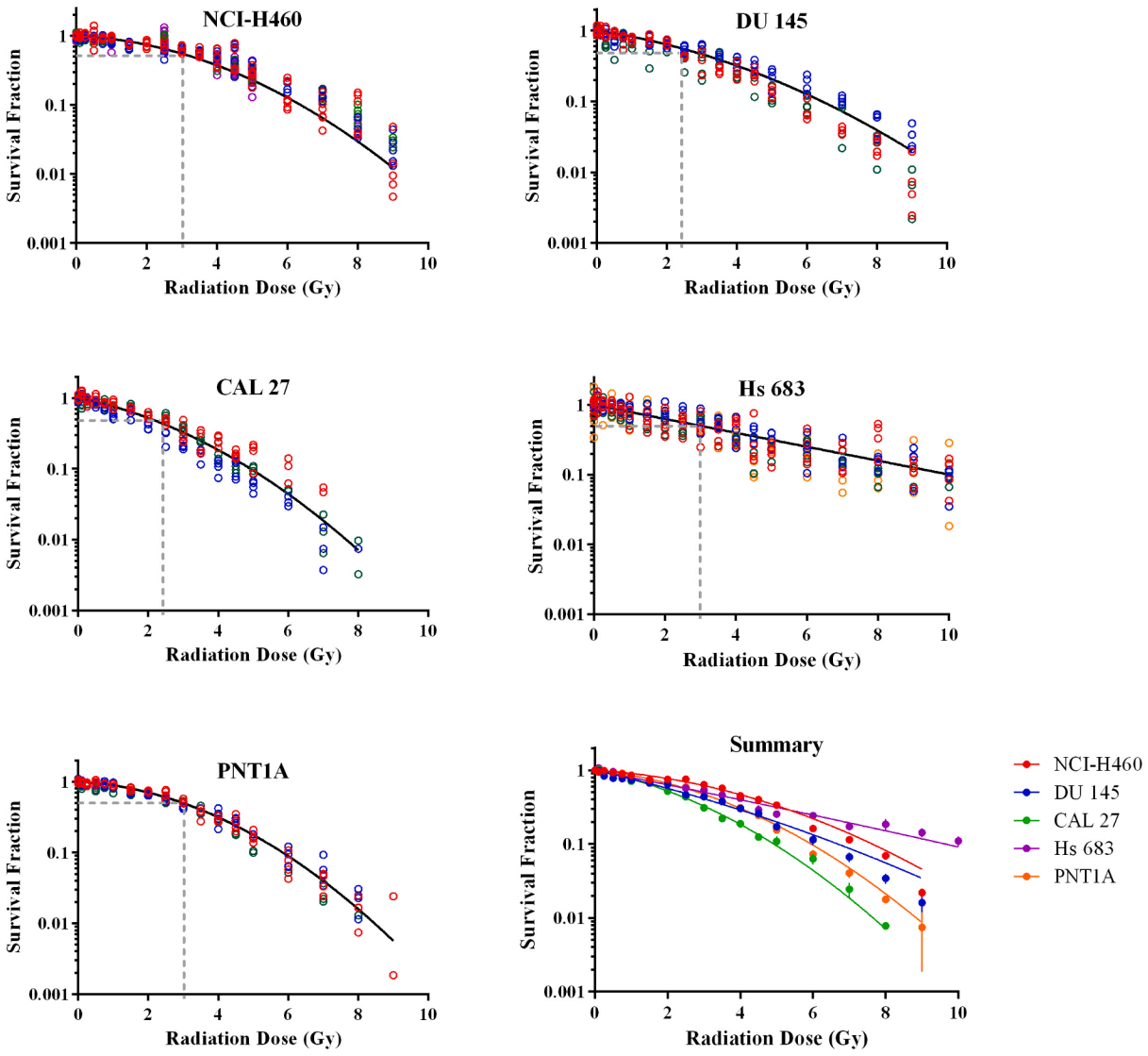

Fig. 2. Dose response curves for each data point represents a flask and colour represents each experiment. The black line indicates the linear-quadratic fit to the data using maximum likelihood. The dose for 0.5 survival fraction, is indicated by dotted lines.

predicted to be 0.2% for all cancer cell lines. Fig. 4 compares this prediction with the observed reduction in survival for all cancer cell lines from an additional CBCT, given by the mean of the distribution of differences in survival fraction, showing that the difference in survival was in the order of 17 times greater than predicted (3.9% measured vs 0.2% predicted, $p < 0.025$). Normal cells alone also showed a larger, 11 times greater, than predicted difference (3.1% measured vs 0.3% predicted), however this was not statistically significant.

4. Discussion

The CBCT dose delivers an additional radiation dose in radiotherapy and until now it was not clear what its biological effect may be. We found, using an in-vitro radiobiology study of cancer cell lines, that a CBCT dose preceding a therapy dose reduced cell survival by more than predicted, with the difference between observed and predicted being significant.

There are three possible interpretations of this finding. First, the imaging dose causes a response, characterised by low dose hyper-radiosensitivity [11], independent of the subsequent therapy dose. Second, the keV CBCT radiation has a higher Relative Biological Effectiveness (RBE) than the MeV therapeutic beam. Third, a radiation induced bystander effect (RIBE) applies, sensitising the cells for a limited time after the CBCT, magnifying the overall reduction in survival [15,22]. If any of these explanations is true, the overall survival fraction cannot be predicted by a simple sum of the imaging and treatment doses. The first and second interpretations predict survival is independent of time delay, while the third predicts it is dependent. We kept the time between the imaging and therapy constant at 3 min and the time between each treatment fields at 1 min. To discriminate between interpretations, a variable time delay between imaging and therapy could be used.

Low dose hyper-radiosensitivity is well documented and the measured CBCT head dose at 0.66 cGy is in the range below 10 cGy where this response is expected [23]. From the radiation dose response survival curves (Fig. 2), testing for the existence of a low dose hyper-radiosensitivity was carried out by combining the 0 Gy and 0.1 Gy survival fractions for all cell lines, but this phenomenon was only observed for lung cancer NCI-H460 ($p = 0.046$) and normal prostate PNT1A ($p = 0.011$). This observation is insufficient to explain our findings.

A range of values for RBE has been reported for low energy beams, motivated by concerns of induced cancers from population screening. RBE for very low doses of radiation, typical of screening and imaging

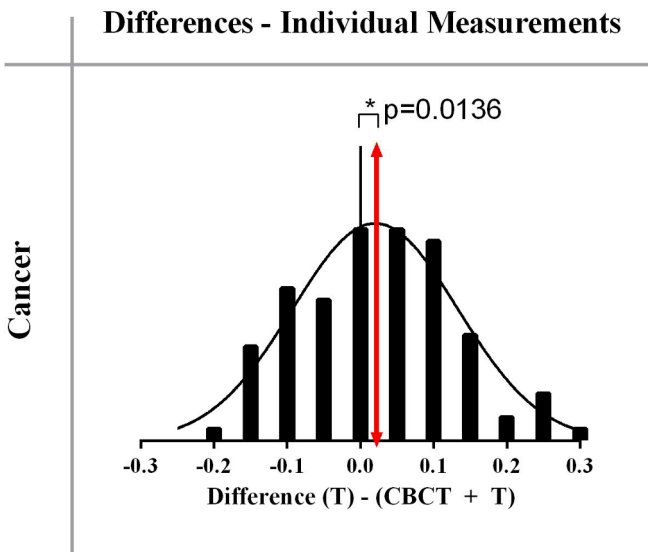

Fig. 3. Frequency distribution (bin width = 0.05) of the difference in survival fractions (T)–(CBCT + T) for all cancer cell lines for individual measurements (n = 103). The distribution of differences passed normality testing using two normality tests (Supplementary Table 2), justifying the use of the paired *t* test (p-values given). The red line represents the mean of the distribution. (For interpretation of the references to colour in this figure legend, the reader is referred to the web version of this article.)

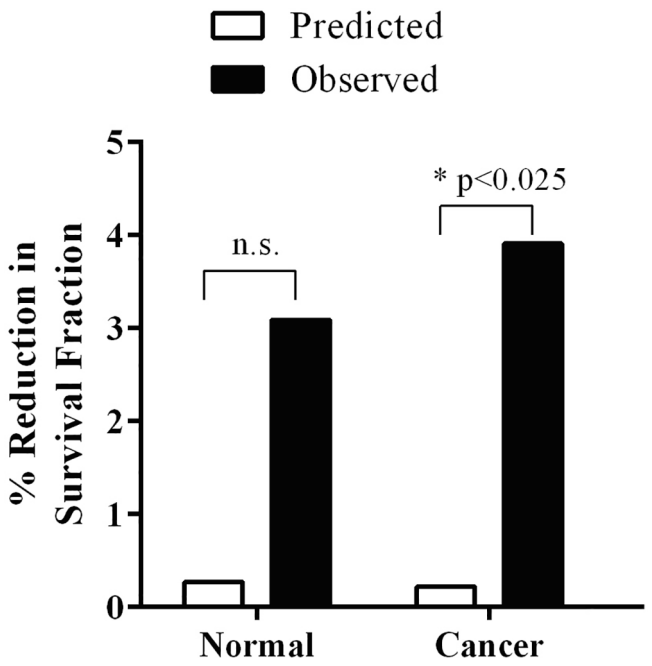

Fig. 4. Predicted and observed reduction in survival as a result of an additional CBCT of 0.66 cGy. Observed reduction is significantly greater than predicted for all cancer cell lines, but was not significantly different for the normal cell line.

exposures, is difficult to measure and many studies lack statistical power. Our CBCT beam has an energy of 100kVp, HVL of 4.9 mm Al. Extrapolating from the data presented by Nikjoo et al. [24] for double strand breaks, the RBE is estimated to be 1.0 for a 6MV photon [25] and 1.11 for 100kVp X-ray beam [26]. This increase in RBE at low energies is also insufficient to explain the observations.

In support of the third interpretation, a study of eleven cell lines Lin and Wu [15] report a dose of<0.5 Gy preceded a larger dose of greater than 1 Gy, causes a greater reduction in survival than the doses given in the reverse order. The smaller dose could be considered as a "priming dose", increasing the sensitivity of the cells to the subsequent larger dose. The CBCT dose stimulates inter- and intra-cellular communication, which fall within the general description of RIBE and are reported to occur above 0.2 to 0.3 cGy [27]. This mechanism has the potential to significantly affect response to the therapy dose and could explain our observations. Peng et al. have recently developed a model that embodies the expression of radiation induced sensitising factors to explain responses to modulated fields [28].

Our prediction is from an *'in-vitro'* study, albeit with high statistical power, and it is not clear how it would translate to clinical practice. We have been able to detect a biological effect of a small imaging dose because of the very large number of individual experiments. A test with similar statistical power would be difficult to replicate in the clinic as it would be challenged by large inter-patient variability.

Our findings have obvious clinical impact. Although it could be argued that the dose from a CBCT is small relative to the therapeutic dose, the response to that dose is in the order of 17 times greater than predicted (3.9% measured vs 0.2% predicted, Fig. 4). Most radiotherapy patients will receive a dose from CBCT in the course of their treatment, usually exposing more than just the target volume, raising concerns of a potential increase in the risk of secondary cancers [29]. The AAPM Task Group 180 addresses the quantification, management and reduction of dose from image guidance [30] and recommend the incorporation of the dose from imaging into the treatment plan should it exceed a threshold value of 5% of the treatment dose. The 5% threshold was based on observed tumour response and morbidity as well as the limited accuracy of therapy dose planning and delivery [31,32]. Our findings favour another approach based on the biological effect rather than simply the dose value from imaging. If this is done, our findings suggest the threshold value of imaging dose for incorporating it into the treatment plan may need to be much lower. We find the dose from a single CBCT is only 0.2% of the therapy dose, but results in a reduction in survival of 3.9% (Fig. 4). A decrease in survival of 3.9% would be caused by an average increase in therapy dose of 6.7%, calculated from the dose response curves of the individual cancer cell lines. Given the trend towards ever-decreasing tumour margins enabled by CBCT, it is not uncommon for repeat imaging to be performed [33]. We are not proposing the omission of CBCT, but we are establishing the radiobiological consequences, when CBCT is delivered in conjunction with a therapeutic fraction.

The next stage may be to perform an in-vivo animal study which would require paired data of identical treatments where one sample group received CBCT and one group would not. For sufficient statistical power it is likely this study would require a large number of animals. Clinically the frequency of CBCT is increased when greater accuracy, smaller margins and higher doses are prescribed, making a clinical study challenging. Furthermore, if a treatment is modified based on information provided by the CBCT, a hidden variable will be introduced to the study. Given the difficulty and the expense of a large in-vivo the findings we present here are unique. Until our research question can be answered in-vivo, it can be argued that the dose from imaging should be evaluated and recorded in the patient record. This record would create an opportunity to subsequently correlate the sequence and magnitude of imaging dose with patient outcomes, for example in local tumour control.

In conclusion, our experimental study led to two key findings: first, the dose from CBCT in addition to the radiation therapy dose causes a measurable reduction in cell survival. Second, the reduction in survival was found to be much larger (~17 times) than predicted by increasing the therapy dose by an amount equal to the CBCT dose (0.66 cGy). This finding is attributed to the radiation-induced bystander effect stimulated by the CBCT dose sensitizing the cells to the subsequent therapy dose. As the use of CBCT is now routine in clinical practice, there is an opportunity to improve the therapeutic outcome by strategically incorporating the enhanced biological response of cancer cells to the CBCT dose

in the calculation of the treatment.

Declaration of Competing Interest

The authors declare that they have no known competing financial interests or personal relationships that could have appeared to influence the work reported in this paper.

Appendix A. Supplementary data

Supplementary data to this article can be found online at https://doi.org/10.1016/j.phro.2020.11.003.

References

[1] Hvid CA, Elstrøm UV, Jensen K, Grau C. Cone-beam computed tomography (CBCT) for adaptive image guided head and neck radiation therapy. Acta Oncol 2018;57:552–6. https://doi.org/10.1080/0284186X.2017.1398414.

[2] Lyons CA, King RB, Osman SOS, McMahon SJ, O'Sullivan JM, Hounsell AR, et al. A novel CBCT-based method for derivation of CTV-PTV margins for prostate and pelvic lymph nodes treated with stereotactic ablative radiotherapy. Radiat Oncol 2017;12:124. https://doi.org/10.1186/s13014-017-0859-z.

[3] Wald PM, Mo X, Barney C, Grecula JC, Williams TM, Haglund KE, et al. Tumor volume dynamics on kV-CBCT during definitive radiation therapy for locally advanced NSCLC: implications for prognosis and adaptive radiation therapy. Int J Radiat Oncol Biol Phys 2017;99:E499–500. https://doi.org/10.1016/j.ijrobp.2017.06.1796.

[4] Tomic N, Devic S, DeBlois F, Seuntjens J. Reference radiochromic film dosimetry in kilovoltage photon beams during CBCT image acquisition. Med Phys 2010;37:1083–92. https://doi.org/10.1118/1.3302140.

[5] Letourneau E, Hinse M, Vallejo CF. Organ dose reduction while using in-house CBCT patient-specific protocols based on OSL dosimetry. Int J Radiat Oncol Biol Phys 2014;90. https://doi.org/10.1016/j.ijrobp.2014.05.2397. S834-8.

[6] Cheng CS, Jong WL, Ung NM, Wong JHD. Evaluation of imaging dose from different image guided systems during head and neck radiotherapy: a phantom study. Radiat Prot Dosim 2017;175:357–62. https://doi.org/10.1093/rpd/ncw357.

[7] Stock M, Palm A, Altendorfer A, Steiner E, Georg D. IGRT induced dose burden for a variety of imaging protocols at two different anatomical sites. Radiother Oncol 2012;102:355–63. https://doi.org/10.1016/j.radonc.2011.10.005.

[8] Alaei P, Ding GX. Image guidance in radiation therapy: techniques, accuracy, and limitations. Am Assoc Physicists Med 2018.

[9] Mijnheer B. In: Clinical 3D dosimetry in modern radiation therapy. first Edition ed. CRC Press; 2017. 674 p..

[10] Alaei P, Ding G, Guan H. Inclusion of the dose from kilovoltage cone beam CT in the radiation therapy treatment plans. Med Phys 2010;37:244–8. https://doi.org/10.1118/1.3271582.

[11] Joiner MC, Marples B, Lambin P, Short SC, Turesson I. Low-dose hypersensitivity: current status and possible mechanisms. Int J Radiat Oncol Biol Phys 2001;49:379–89. https://doi.org/10.1016/S0360-3016(00)01471-1.

[12] Short SC, Bourne S, Martindale C, Woodcock M, Jackson SP. DNA damage responses at low radiation doses. Radiat Res 2005;164:292–302. https://doi.org/10.1667/RR3421.1.

[13] Suzuki K, Kodama S, Watanabe M. Extremely low-dose ionizing radiation causes activation of mitogen-activated protein kinase pathway and enhances proliferation of normal human diploid cells. Cancer Res 2001;61:5396–401. http://search.proquest.com/docview/71016133/.

[14] Feinendegen LE. Evidence for beneficial low level radiation effects and radiation hormesis. Br J Radiol 2005;78:3–7. https://doi.org/10.1259/bjr/63353075.

[15] Lin PS, Wu A. Not all 2 Gray radiation prescriptions are equivalent: cytotoxic effect depends on delivery sequences of partial fractionated doses. Int J Radiat Oncol Biol Phys 2005;63:536–44. https://doi.org/10.1016/j.ijrobp.2005.06.010.

[16] Yan J, Yang J, Yang Y, Ren W, Liu J, Gao S, et al. Use of pulsed low-dose rate radiotherapy in refractory malignancies. Transl Oncol 2018;11:175–81. https://doi.org/10.1016/j.tranon.2017.12.004.

[17] Rogers LJ, Suchowerska N, Ralston A, Napper A, McKenzie DR. Imaging dose affects *in vitro* survival following subsequent therapeutic irradiation. BPEX 2015;1:045016. https://doi.org/10.1088/2057-1976/1/4/045016.

[18] Potter MD, Suchowerska N, Rizvi S, McKenzie DR. Hidden stressors in the clonogenic assay used in radiobiology experiments. Australas Phys Eng Sci Med 2011;34:345–50. https://doi.org/10.1007/s13246-011-0082-4.

[19] Franken NA, Rodermond HM, Stap J, Haveman J, van Bree C. Clonogenic assay of cells in vitro. Nat Protoc 2006;1:2315–9. https://doi.org/10.1038/nprot.2006.339.

[20] Claridge Mackonis E, Suchowerska N, Naseri P, McKenzie DR. Optimisation of exposure conditions for in vitro radiobiology experiments. Australas Phys Eng Sci Med 2012;35:151–7. https://doi.org/10.1007/s13246-012-0132-6.

[21] Braselmann H, Michna A, Hess J, Unger K. CFAssay: statistical analysis of the colony formation assay. Radiat Oncol 2015;10:223. https://doi.org/10.1186/s13014-015-0529-y.

[22] Peng V, Suchowerska N, Rogers L, Claridge Mackonis E, Oakes S, McKenzie DR. Grid therapy using high definition multileaf collimators: realizing benefits of the bystander effect. Acta Oncol 2017;56:1048–59. https://doi.org/10.1080/0284186x.2017.1299939.

[23] Basic clinical radiobiology. 3rd ed. ed. Steel GG, editor. London: Arnold; 2002.

[24] Nikjoo H, Lindborg L. RBE of low energy electrons and photons. Phys Med Biol 2010;55:R65–109. https://doi.org/10.1088/0031-9155/55/10/r01.

[25] Friedland W, Jacob P, Paretzke HG, Merzagora M, Ottolenghi A. Simulation of DNA fragment distributions after irradiation with photons. Radiat Environ Biophys 1999;38:39–47. https://doi.org/10.1007/s004110050136.

[26] Hsiao Y, Stewart RD. Monte Carlo simulation of DNA damage induction by x-rays and selected radioisotopes. Phys Med Biol 2008;53:233–44. http://doi.org//0031-9155/53/1/016.

[27] Tomita M, Maeda M. Mechanisms and biological importance of photon-induced bystander responses: do they have an impact on low-dose radiation responses. J Radiat Res 2015;56:205–19. https://doi.org/10.1093/jrr/rru099.

[28] Peng V, Suchowerska N, Esteves ADS, Rogers L, Claridge Mackonis E, Toohey J, et al. Models for the bystander effect in gradient radiation fields: range and signalling type. J Theor Biol 2018;455:16–25. https://doi.org/10.1016/j.jtbi.2018.06.027.

[29] Hoang JK, Reiman RE, Nguyen GB, Januzis N, Chin BB, Lowry C, et al. Lifetime attributable risk of cancer from radiation exposure during parathyroid imaging: comparison of 4D CT and parathyroid scintigraphy. Am J Roentgenol 2015;204:W579–85. https://doi.org/10.2214/ajr.14.13278.

[30] Ding GX, Alaei P, Curran B, Flynn R, Gossman M, Mackie TR, et al. Image guidance doses delivered during radiotherapy: Quantification, management, and reduction: report of the AAPM Therapy Physics Committee Task Group 180. Med Phys 2018;45:e84–99. https://doi.org/10.1002/mp.12824.

[31] Landberg T, Chavaudra J, Dobbs J, Gerard J-P, Hanks G, Horiot J-C, et al. Report 62. J of the international commission on radiat units and measurements. 2016;os32:NP. http://doi.org/10.1093/jicru/os32.1.Report62.

[32] Dische S, Saunders MI, Williams C, Hopkins A, Aird E. Precision in reporting the dose given in a course of radiotherapy. Radiother Oncol 1993;29:287–93. https://doi.org/10.1016/0167-8140(93)90146-y.

[33] Obedian E, Capece D, Kapoor D, Zimberg SH. The value of repeat cone beam CT scans in image guided radiation therapy for prostate cancer. Int J Radiat Oncol Biol Phys 2012;84:S768. https://doi.org/10.1016/j.ijrobp.2012.07.2056.